Quantum Hall Ferrimagnetism in Lateral Quantum Dot Molecules

Ramin M. Abolfath* and Pawel Hawrylak

Institute for Microstructural Sciences, National Research Council of Canada, Ottawa, K1A 0R6, Canada

(Received 21 July 2006; published 1 November 2006)

We demonstrate the existence of ferrimagnetic and ferromagnetic phases in a spin phase diagram of coupled lateral quantum dot molecules in the quantum Hall regime. The spin phase diagram is determined from the Hartree-Fock configuration interaction method as a function of electon number N and magnetic field B. The quantum Hall ferrimagnetic phase corresponds to spatially imbalanced spin droplets resulting from strong interdot coupling of identical dots. The quantum Hall ferromagnetic phases correspond to ferromagnetic coupling of spin polarization at filling factors between $\nu = 2$ and $\nu = 1$.

DOI: 10.1103/PhysRevLett.97.186802 PACS numbers: 73.43.Lp, 73.63.Kv, 75.50.Gg

Electron-electron interactions are responsible for the magnetic properties of solids [1,2]. It is now possible to engineer the many-body states of electrons by confining them in artificially fabricated nanostructures to control their magnetic properties [3–5]. This has been demonstrated in quantum wells [6] and dots where, by varying the magnetic field, the total electron spin has been tuned from $S = 0$ at a spin singlet quantum Hall droplet at filling factor $\nu = 2$ to the maximally spin polarized ferromagnetic filling factor $\nu = 1$ droplet [7–9]. More complex spin textures associated with correlated states such as spin biexcitons were also identified and observed experimentally [10].

Given the tunability of the total spin with magnetic field and electron numbers in a single dot, it is natural to explore the possibility of magnetic coupling in quantum dot molecules [11–17]. In this Letter we explore the effect of magnetic field, interdot tunneling, and electron-electron interactions on the evolution of total electron spin for different electron numbers in a lateral quantum dot molecule. The interdot and intradot electron-electron Coulomb interactions are incorporated systematically using the Hartree-Fock configuration interaction method (HF-CI). We find quantum Hall droplets with zero and full spin polarization, identified as $\nu = 2$ and $\nu = 1$ quantum Hall droplets in analogy with single quantum dots and quantum Hall ferromagnetism [6]. Between these two states, we find a series of continuous transitions among partially spin polarized phases. Simultaneous spin flips in each isolated dot must lead to an even number of spin flips in a double dot. Surprisingly, we find partially polarized phases with an odd number of spin flips. We identify these correlated states as quantum Hall *ferrimagnets* [2,18], which are a direct manifestation of coherent quantum mechanical coupling between the quantum dots as well as interdot electronic correlations.

We describe electrons confined in a quasi-two-dimensional quantum dot molecule in a uniform perpendicular magnetic field by the effective mass Hamiltonian $H = \sum_{i=1}^{N} T_i + \frac{e^2}{2\epsilon}\sum_{i\neq j}\frac{1}{|\vec{r}_i - \vec{r}_j|} + E_Z$, where $T = \frac{1}{2m^*}[\frac{\hbar}{i}\vec{\nabla} + \frac{e}{c}A(\vec{r})]^2 + V(x, y)$ is the single electron Hamiltonian in the magnetic field. Here $(\vec{r}) = (x, y)$ describes the electron position, $A(\vec{r}) = \frac{1}{2}\vec{B} \times \vec{r}$ is the magnetic vector potential, and m^* is the conduction-electron effective mass, e is the electron charge, and ϵ is the host semiconductor dielectric constant ($\epsilon = 12.8$ in GaAs). $E_Z = \gamma\omega_c$ is the Zeeman energy, $\sigma = +1(-1)$ corresponds to spin $\uparrow$ ($\downarrow$), $\gamma = m^* g$, g is the host semiconductor g factor ($g = -0.44$ in GaAs and $g = -14$ in InAs), and μ_B is the Bohr magneton. $V(\vec{r})$ is the quantum dot molecule confining potential, parameterized in terms of a sum of three Gaussians $V(x, y) = V_0 \exp[-\frac{(x+a)^2+y^2}{\Delta^2}] + V_0 \exp[-\frac{(x-a)^2+y^2}{\Delta^2}] + V_p \exp[-\frac{x^2}{\Delta_{Px}^2} - \frac{y^2}{\Delta_{Py}^2}]$. Here, V_p is the central plunger gate potential controlling the tunneling barrier. The parameters $V_0 = -10$, $\Delta = 2.5$, $a = 2$, and $\Delta_{Px} = 0.3$, $\Delta_{Py} = 2.5$ in effective atomic units describe a typical confining potential corresponding to weakly coupled quantum dots. Diagonalizing the single particle Hamiltonian as in Ref. [16] we obtain the single particle spectrum as a function of magnetic field shown in Fig. 1. In order to illustrate the physics of spin flips in a coupled molecule, the spectrum corresponds to a large Zeeman coupling. At zero magnetic field it exhibits well separated s, p, and d electronic shells, and at high magnetic fields it forms the lowest Landau level (LLL) molecular shells of closely spaced pairs of bonding-antibonding orbitals. In a high magnetic field the corresponding wave functions admit a description in terms of localized LLL orbitals [16]. In this limit linear combinations of the LLL orbitals m from left and right dot form molecular shells of closely spaced symmetric (S) antisymmetric (A) pairs with eigenenergies expressed approximately as $\epsilon_{m\lambda\sigma} = \omega_-(m + \frac{1}{2}) - \lambda\frac{\Delta_m}{2} - \frac{1}{2}\sigma\gamma\omega_c$, where $\omega_- = \sqrt{\omega_0^2 + \omega_c^2/4} - \omega_c/2$ (Fock-Darwin eigenenergies of a parabolic dot), and $\omega_0 = 2\sqrt{|V_0|/\Delta^2}$ [16]. Here λ is the pseudospin index, the symmetric (antisymmetric) orbitals labeled by $\lambda = +1(-1)$. Δ_m is the symmetric-antisymmetric gap. These orbitals can be grouped into electronic shells, depending on the number of electrons. The half-filled molecular shells correspond to

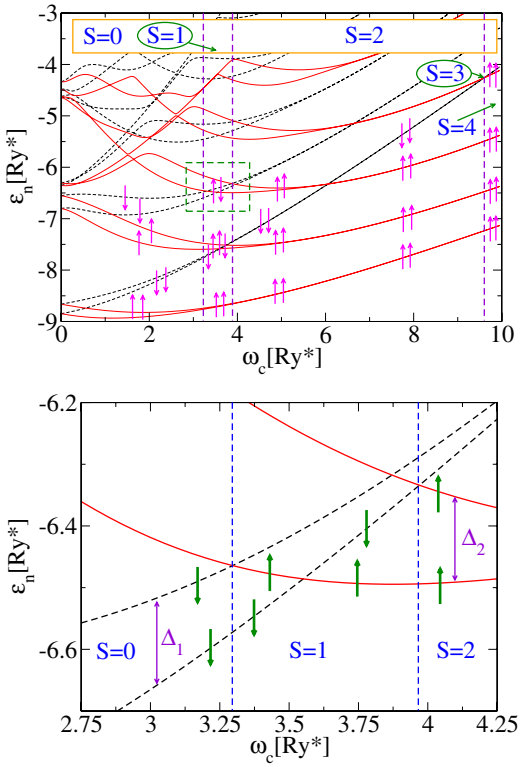

FIG. 1 (color online). Double dot single particle spectrum in the presence of Zeeman coupling. For illustration purposes a very high Zeeman coupling $g = -9$ was used. The inset shows the evolution of total spin as a function of magnetic field in a quantum dot molecule with $N = 8$ noninteracting electrons. The states surrounded by circles show odd spin. The stability range of these states is very narrow due to small interdot tunneling amplitude. The bottom is the enlarged part of the spectrum (the box in the top) which shows the evolution of first and second spin flip transitions.

electron numbers ($N_L = 2k - 1$, $N_R = 2k - 1$) and filled shells correspond to ($N_L = 2k$, $N_R = 2k$) configurations (k is the integer).

In Fig. 1 the $S_z = 0$, 2, and 4 phases of the $N = 8$ electron droplet are shown. They are obtained by occupying the lowest single particle energy levels. The even S_z phases can be understood as simultaneous spin flips in each isolated dot. However, we see in Fig. 1 also odd S_z phases. In the bottom part of Fig. 1 the first odd spin $S_z = 1$ state occurs between magnetic fields corresponding to $\omega_c(1) \approx 3.25$ and $\omega_c(2) \approx 3.9$, which in turn corresponds to the crossing of energy levels $\epsilon_{m=2,\sigma=\uparrow,\lambda=+1} = \epsilon_{m=1,\sigma=\downarrow,\lambda=-1}$, and $\epsilon_{m=2,\sigma=\uparrow,\lambda=-1} = \epsilon_{m=1,\sigma=\downarrow,\lambda=+1}$. Using single particle eigenenergies, we find the stability range of the odd spin phase directly related to the tunneling splitting of energy levels: $\gamma[\omega_c(2) - \omega_c(1)] = [\Delta_2(2) + \Delta_1(2)]/2 + [\Delta_2(1) + \Delta_1(1)]/2$. Hence the odd spin flip state is related to the splitting of energy levels due to tunneling: States with $S_z = 1$, and $S_z = 3$, are stable within the narrow range of magnetic fields due to spin flip transitions among the electrons that occupy the levels with energy separation proportional to the interdot tunneling amplitude. This is in contrast with the first spin flip transition in single dots, which is stable in a wide range of magnetic fields. For this reason the existence and stability range of odd spin states in the spin phase diagram of quantum dot molecules can be interpreted as the measure of interdot interaction.

The above analysis emphasizes the relationship between odd spin phases and quantum mechanical coupling between the dots. This coupling in single dots is not due to single particle effects but due to electron-electron interaction. Hence, we now turn off Zeeman coupling and analyze the effects of electron-electron interactions on spin transitions. We focus on the tunnel coupled lowest Landau level orbitals m. The $\nu = 2$ state of quantum dot molecule with N electrons and total spin $S = 0$ is shown in Fig. 2. The energy associated with this state $E_{\nu=2} = \sum_{m=0}^{N/4-1} \sum_{\lambda=\pm1} \sum_{\sigma} [\epsilon_{m\lambda\sigma} + \Sigma(m, \lambda, \sigma)]$ can be expressed in terms of electron self-energy $\Sigma(m, \lambda, \sigma)$. The $S = 1$ spin flip excitation is constructed by removing an electron from occupied $\nu = 2$ state and putting into an unoccupied state. There are two possible spin excitons for a given parity, depicted in Fig. 2, A to S (AS) and S to A (SA). Figure 2 (bottom) shows the numerically calculated energies of spin excitons in the $N = 8$ electron droplet as a function of magnetic field. The energy $\Delta E_{X_{\mathrm{AS}}}$ of spin exciton X_{AS} is positive for magnetic fields shown but the energy $\Delta E_{X_{\mathrm{SA}}}$ of spin exciton X_{SA} becomes negative at $\omega_c = 3.8$, i.e., the X_{SA} spin flip state becomes the lower energy state than the $\nu = 2$, $S = 0$ state. However, in stark contrast with a single quantum dot, we find that the second spin flip state XX becomes the ground state at lower magnetic field $\omega_c = 2.1$. Hence, unlike in a single quantum dot we find a transition from the spin singlet $S = 0$ state directly to the $S = 2$ second spin flip state. This is a transition corresponding to even total spin numbers, as if the two dots were flipping their spin simultaneously. However, the two spin excitons X_{AS} and X_{SA} are not eigenstates of the Hamiltonian and are coupled by Coulomb interaction. The resulting energy $\Delta E_{X_{\mathrm{SA}}+X_{\mathrm{AS}}}$ of the correlated single spin state is significantly lower and equals both the energy ΔE_{XX} of the second spin flip biexciton and of the $\nu = 2$, $S = 0$ state at $\omega_c = 2.1$. At this magnetic field the energy of the biexciton and of the exciton are almost identical. The $S = 1$ states show stability in a narrow range of magnetic field, within the accuracy of our numerical results. With further increase of magnetic field, single excitons condense into pairs of excitons forming biexcitons. The existence of single, odd, spin excitons is hence a signature of electronic correlations. These states can be thought of as follows: one of the quantum dots underwent spin transition and the excess spin tunneled back and forth between the two dots. The correlated odd spin state does not exist at the Hartree-Fock level as shown above and can be identified as the quantum Hall ferrimagnet.

To support the assertion that correlations are responsible for the existence of odd spin excitons, we employ the HF-CI method to calculate the ground state properties of

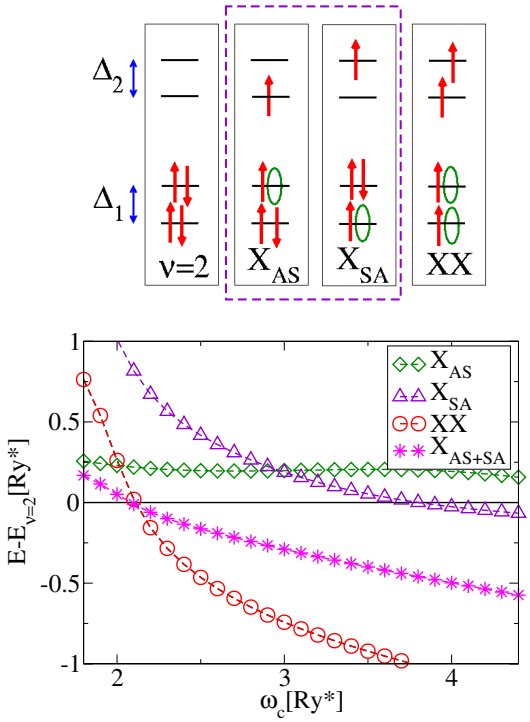

FIG. 2 (color online). (Top) The basis of spin configurations in high magnetic fields. The first spin transition states $S = 1$ identify with two independent set: $\{X_{SS}, X_{AA}\}$, and $\{X_{SA}, X_{AS}\}$. In the former the electron-hole transitions occurs between the states with the same symmetry and hence they do not mix with the latter which exhibit the process of electron-hole excitations between states with opposite parity. (Bottom) The energies of two single spin excitons X_{SA} and X_{AS} with odd parity, the energy of the odd parity correlated exciton X_{SA+AS}, and the energy of the spin biexciton $S = 2$ state as a function of magnetic field. All energies measured from the energy of the $\nu = 2$, $S = 0$ state.

quantum dot molecules in a magnetic field and with electron numbers up to $N = 12$. The HF basis is used for the construction of multielectron configurations, which in turn are used for the construction of the Hamiltonian matrix. The Hamiltonian matrix is either diagonalized exactly for small systems, or low energy eigenvalues and eigenstates are extracted approximately for very large number of configurations ($\approx 10^7$) [19]. Figure 3 shows the evolution of total spin and the energy gap with increasing magnetic field in $N = 8$ quantum dot molecule. For comparison the spin evolution of two noninteracting $N = 4$ quantum dots is shown with a dashed line. We find that the effect of direct, exchange, and correlation energies calculated by HF-CI is to renormalize the magnetic fields at which spin transitions take place, and more importantly, to lead to the appearance of odd spin states $S = 1$ and $S = 3$, in agreement with our previous analysis.

While the existence of odd spin states is most striking, the presence of spin polarized phases is also nontrivial. The fact that spins of electrons on two quantum dots align demonstrates the existence of ferromagnetic dot-dot coupling. In the case of antiferromagnetic coupling there

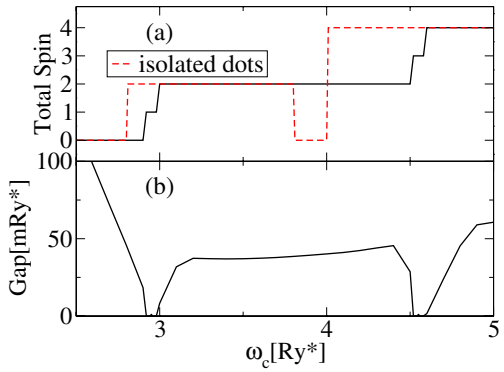

FIG. 3 (color online). (a) The evolution of spin of the $N = 8$ electron quantum dot molecules as a function of magnetic field for $\gamma = -0.02$ and $V_p = 7$ (solid line). For comparison the spin evolution of two isolated dots with $\gamma = -0.02$ is shown (dashed line). (b) The evolution of the energy gap of the quantum dot molecules as a function of magnetic field.

would have been no net spin even though each dot has finite spin. As shown in Fig. 1 without electron-electron interactions competition between quantum mechanical tunneling and Zeeman energy was responsible for the existence of odd spin phases. The effect of finite Zeeman energy is similar in an interacting system. The effect of increasing Zeeman energy on the evolution of spin and energy gap of the N-electron quantum dot molecules as a function of magnetic field is to renormalize the magnetic field value of spin flips and, more importantly, to stabilize the odd spin phases.

Here we summarize our results for other even electron numbers, $N = 2$, 4, 6, 8, 10, and 12, in the form of a phase diagram shown in Fig. 4. The details of our calculation and complete phase diagram as a function of Zeeman energy and tunneling barrier height will be presented elsewhere [20]. The tunneling barrier and Zeeman coupling are $V_p = 7$ and $\gamma = -0.02$. With the choice of electron numbers the phase diagram covers quantum molecules build out of artificial atoms with up to second filled shell. For example,

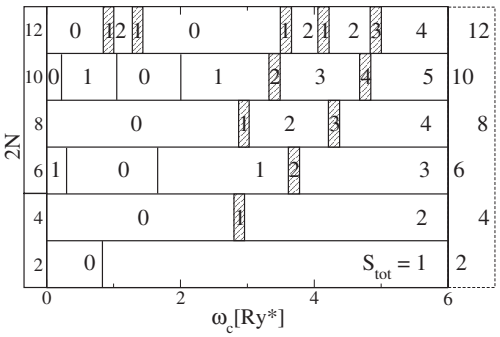

FIG. 4. Spin phase diagram of artificially coupled dots molecules in the presence of Zeeman coupling with $\gamma = -0.02$ and tunneling barrier $V_p = 7$. Numbers in blocks represent the total spin. Shaded areas show the stability region of ferrimagnetic states.

the $N = 4$ molecule corresponds to two quantum dots (2,2), each with a filled s shell. The $N = 12$ molecule is built of two quantum dots (6,6), each with a filled p and s shell. Intermediate electron numbers correspond to molecules built out of artificial atoms with partially filled shells. Partial shell filling implies the Hund rules and total electron spin, e.g., $S = 1$ for a four electron quantum dot. When the two dots (4,4) with four electrons each are brought together into an $N = 8$ electron molecule, the total electron spin of the ground state is found to be $S = 0$, as seen in Fig. 4. But when the two dots (3,3) with three electrons each are brought together into $N = 6$ electron molecule, the total electron spin of the ground state is $S = 1$. Hence at zero magnetic field there exists a rich phase diagram sensitive to the separation of the two dots and the barrier height. The situation is significantly simplified by the application of the magnetic field. For all electron numbers the increasing magnetic field forces electrons to flip the spin and increase spin polarization until all electron spins are aligned. In the phase diagram the spin polarized phase with $S = N/2$ is visible. This phase can be attributed to the ferromagnetic $\nu = 1$ quantum Hall droplets. The spin transitions leading to the spin polarized droplet do depend on the number of electrons. We discuss below the nature of the magnetic field induced spin transitions for half-filled shells of coupled dots with $(N_L + 1, N_R + 1)$ electron numbers. The half-filled shells correspond to filled shells and the additional electron in each dot. For (1,1) there are only $N = 2$ electrons and one finds the singlet at low magnetic fields followed by a triplet at higher magnetic fields. For higher electron numbers the system can be interpreted as effective two-electron ($N_L = 1, N_R = 1$) artificial molecules, with $S = 0$ core electrons ($S_L = 0$, $S_R = 0$) and finite spin valence electrons with antiferromagnetic/ferromagnetic coupling, corresponding to the spin singlet $|\uparrow\downarrow\rangle - |\downarrow\uparrow\rangle$ and spin triplet $|\uparrow\uparrow\rangle$ [14,16] states. Thus the corresponding Hamiltonian can be reduced to the Heisenberg model $H = JS_LS_R$ by restricting the valence electrons to a two level model (Hund-Mullikan approximation), and by extension of the half-filled Hubbard model. Here S_L and S_R are the spin-1/2 operator for the two localized valence electrons, and J is the singlet-triplet splitting. The spin singlet $S = 0$ state, visible in the phase diagram of Fig. 4 corresponds to filling factor $\nu = 2$ quantum Hall droplets. Finally, in Fig. 4 small domains of quantum Hall ferrimagnetism with $S =$ (even) and $S =$ (odd) corresponding to half-filled and filled shells, stabilized by Zeeman energy, are shown. The half-filled shells with S even can be easily understood. For example, for $N = 10$ the $S = 2$ phase corresponds to $S = 1/2$ on one dot and $S = 3/2$ on a second dot; i.e., only the second dot underwent a spin flip.

In conclusion, we have presented the spin phase diagram of quantum dot artificial molecules for different numbers of electrons as a function of the external magnetic field. The phase diagram was obtained using the Hartree-Fock configuration interaction method. The magnetic field allows the tuning of the total spin of electrons in each artificial atom. Quantum mechanical tunneling and electron-electron interactions couple spins of each artificial atom and result in ferromagnetic and antiferromagnetic states tunable by the magnetic field and barrier potential. Rather surprisingly, ferrimagnetic states in which one of the dots undergoes spontaneous change of spin were found and predicted.

Authors acknowledge the support by the NRC High Performance Computing Project and by the Canadian Institute for Advanced Research.

*Present address: Department of Physics, SUNY at Buffalo, Buffalo, NY 14260, USA.
Electronic address: abolfath@buffalo.edu

[1] D. C. Mattis, *The Theory of Magnetism, Statics and Dynamics*, Springer-Verlag Series in Solid State Sciences (Springer-Verlag, Berlin–New York, 1981), Vol. I.
[2] James Smart, *Effective Field Theories of Magnetism* (Saunders, Philadelphia, 1966).
[3] M. Ohno *et al.*, Nature (London) **408**, 944 (2000).
[4] A. Sachrajda, P. Hawrylak, and M. Ciorga, in *Transport in Quantum Dots*, edited by J. Bird (Kluwer, Dordrecht, 2003), Chap. 3.
[5] J. Seufert *et al.*, Phys. Rev. Lett. **88**, 027402 (2001); L. Besombes *et al.*, Phys. Rev. Lett. **93**, 207403 (2004); J. Fernández-Rossier and L. Brey, Phys. Rev. Lett. **93**, 117201 (2004); F. Qu and P. Hawrylak, Phys. Rev. Lett. **96**, 157201 (2006).
[6] S. M. Girvin and A. H. MacDonald, in *Perspectives in Quantum Hall Effects: Novel Quantum Liquids in Low-Dimensional Semiconductor Structures*, edited by S. Das Sarma and A. Pinczuk (Wiley, New York, 1997).
[7] S. Tarucha *et al.*, Phys. Rev. Lett. **77**, 3613 (1996).
[8] M. Ciorga *et al.*, Phys. Rev. Lett. **88**, 256804 (2002).
[9] R. Hanson *et al.*, Phys. Rev. Lett. **91**, 196802 (2003).
[10] M. Korkusinski *et al.*, Phys. Rev. Lett. **93**, 206806 (2004).
[11] J. J. Palacios and P. Hawrylak, Phys. Rev. B **51**, 1769 (1995).
[12] W. G. van der Wiel *et al.*, Rev. Mod. Phys. **75**, 1 (2002).
[13] S. M. Reimann and M. Manninen, Rev. Mod. Phys. **74**, 1283 (2002).
[14] M. Pioro-Ladriere *et al.*, Phys. Rev. Lett. **91**, 026803 (2003).
[15] T. Hatano *et al.*, Phys. Rev. Lett. **93**, 066806 (2004).
[16] Ramin M. Abolfath, W. Dybalski, and Pawel Hawrylak, Phys. Rev. B **73**, 075314 (2006).
[17] J. R. Petta *et al.*, Science **309**, 2180 (2005).
[18] K. Maisinger *et al.*, Phys. Rev. B **58**, R5908 (1998); M. Abolfath, H. Hamidian, and A. Langari, cond-mat/9901063, and references therein.
[19] R. M. Abolfath and P. Hawrylak, J. Chem. Phys. **125**, 034707 (2006).
[20] R. M. Abolfath and P. Hawrylak (to be published).